

Article

## On Metropolis Integrators for Molecular Dynamics

Nawaf Bou-Rabee <sup>1,\*</sup>

<sup>1</sup> Department of Mathematical Sciences, Rutgers University–Camden, 311 N 5th Street, Camden, NJ 08102, USA

Received: xx / Accepted: xx / Published: xx

---

**Abstract:** This paper invites the reader to experiment with an easy-to-use MATLAB [1] implementation of Metropolis integrators for Molecular Dynamics (MD) simulation [2,3]. These integrators are analysis-based, in the sense that they can rigorously simulate dynamics along an infinitely long MD trajectory. Among explicit integrators for MD, they seem to be the only ones that satisfy the fundamental requirement of stability. The schemes can handle stiff or hard-core potentials, and are straightforward to set up, apply and extend to new situations. Potential pitfalls in high dimension are discussed, and tricks for mitigation are given.

**Keywords:** explicit integrators; Metropolis-Hastings algorithm; ergodicity; weak accuracy

**Classification:** MSC 82C80 (Primary); 82C31, 65C30, 65C05 (Secondary)

---

### 1. Introduction

Molecular Dynamics (MD) simulation refers to the time integration of Hamilton's equations often coupled to a heat or pressure bath [4–8]. From its early use in computing equilibrium dynamics of homogeneous molecular systems [9–16] and pico to nanoscale protein dynamics [17–26], the method has evolved into a general purpose tool for simulating statistical properties of heterogeneous molecular systems [27]. Accessible time horizons have increased remarkably: the timeline in Figure 1 attempts to capture this nearly billion-fold improvement in capability over the last forty or so years. Near future applications include micro to milliscale simulations of biomolecular processes like protein folding, ligand binding, membrane transport, and biopolymer conformational changes [28–30]. In addition, atomistic MD simulations are used more sparingly in multiscale models [31–35] and rare event simulation such as the finite temperature string method and milestoning [36–39]. Given this continuous

development and generalization of MD, it is not a stretch to suppose that MD will play a transformative role in medicine, technology, and education in the twenty-first century.

In its standard form, the method inputs a random initial condition, fudge factors, physical and numerical parameters; and, outputs a long discrete path of the molecular system. Statistical quantities, like velocity correlation or mean radius of gyration, are usually computed online, i.e., as points along this trajectory are produced. MD simulation is built atop a forward Euler-like integrator that requires a single interatomic force field evaluation per step. Even though MD sounds quite simple, software implementations of MD are typically optimized for performance [40–42], and as a side effect, obscure this simplicity and make it cumbersome for newcomers to learn, modify, test and propose enhancements.

Besides this steep learning curve, due to the interplay between stochastic Brownian and interatomic forces, current MD integrators are unable to stably produce long trajectories. This is a well known difficulty with explicit integrators for nonlinear diffusions [43–47]. Recently, a probabilistic solution to this problem was proposed that challenges the traditional notion that Monte-Carlo methods and MD have disjoint aims: the former strictly samples probability distributions and the latter estimates dynamics. The basic idea is to combine a standard MD integrator with a Metropolis-Hastings algorithm targeted to the Gibbs-Boltzmann distribution [2,3,48]. Because the scheme is a Monte-Carlo method it exactly preserves the Gibbs-Boltzmann distribution [2,48]. This important property implies numerical stability over long-time simulations. In addition, a Metropolized integrator is also accurate on finite time intervals [2], and so, even though a Metropolized integrator involves a Monte-Carlo step, its aim and philosophy are very different from Monte-Carlo methods whose only goal is to sample a target distribution with no concern for the dynamics [48–57].

Motivated by these issues, this paper builds a software implementation of a ‘Metropolis integrator’ and applies it to a homogeneous molecular system. The algorithms are introduced in a step-by-step fashion. The software version of the algorithm is written in the latest version of MATLAB with plenty of comments, variables that are descriptively named, and operations that can be easily translated into mathematical expressions [1]. Since MATLAB is widely available, this design ensures the software will be easy-to-use and cross-platform. The following MATLAB-specific file formats will be used.

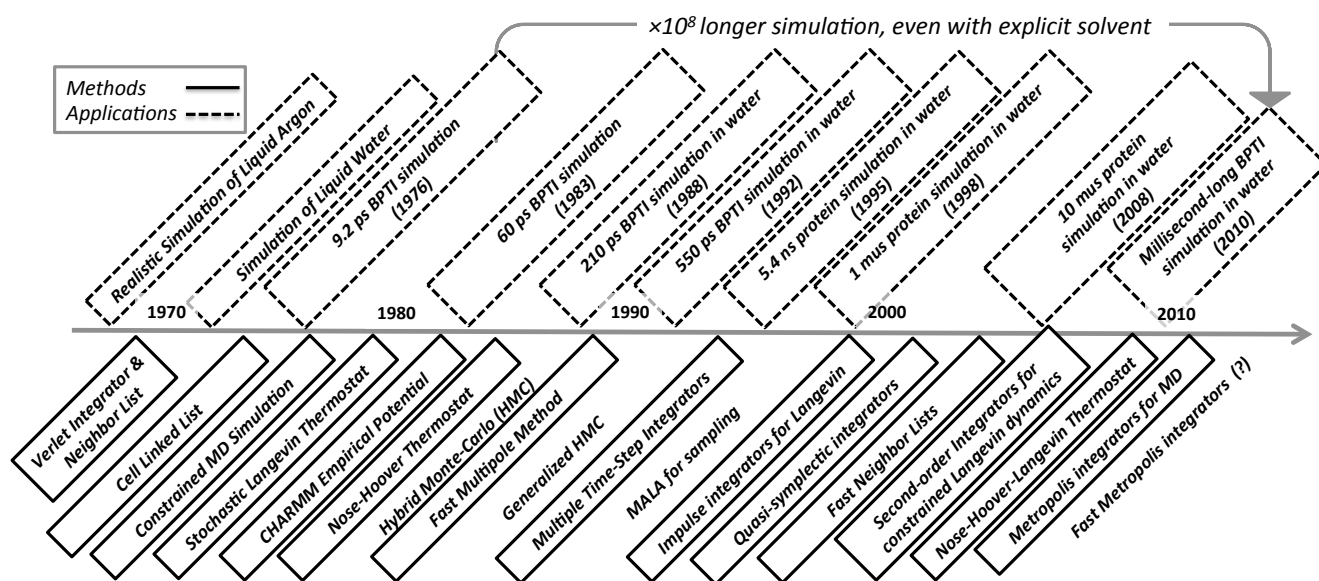
**(F1) MATLAB Script & Function** files are written in the MATLAB language, and can be run from the MATLAB command line without ever compiling them.

**(F2) MATLAB Executable (MEX)** files are written in the ‘C’ language and compiled using the MATLAB `mex` function. The resulting executable is comparable in efficiency to a ‘C’ code and can be called directly from the MATLAB command line. We will use MEX-files for performance-critical routines [58].

**(F3) MATLAB Binary (MAT)** files will be used to store simulation data.

The paper is organized as follows. We begin with some mathematical background in §2, followed by an algorithmic introduction to time integrators in MD simulation and a statistical analysis of a long trajectory of a Lennard-Jones fluid in §3. The paper discusses some tricks to get the integrator to scale well in high dimension in §4. We close the paper with some steps for future development of Metropolis integrators in §5.

**Figure 1. Timeline of Selected MD Developments.** A timeline of the evolution of MD simulation methodology and applications. The applications highlighted are simulations of liquid argon [9], water [14], protein dynamics without solvent [17,18], and biopolymer dynamics with solvent [59–65]. The methods include the following upgrades to MD simulation: Verlet integrator and neighbor lists [10], cell linked list [66], SHAKE integrator for constraints [67], stochastic heat baths via Langevin dynamics [68,69], library of empirical potentials [40], extended/deterministic heat bath via Nosé-Hoover dynamics [70,71], fast multipole method [72], multiple time-steps [73], Langevin splitting methods [74,75], (fast) combined neighbor and cell lists [76], second-order Langevin integrators for constrained systems [77], and stochastic Nosé-Hoover Langevin thermostat [78–80].



## 2. Mathematical Background

### 2.1. Bath-Free Dynamics

MD is based on Hamilton’s equations for a Hamiltonian  $H : \mathbb{R}^{2d} \rightarrow \mathbb{R}$ :

$$\dot{z}(t) = \mathbf{J}\nabla H(z(t)), \quad z(0) \in \mathbb{R}^{2d}, \quad (1)$$

where  $z(t) = (\mathbf{q}(t), \mathbf{p}(t))$  is a vector of molecular positions  $\mathbf{q}(t) \in \mathbb{R}^d$  and momenta  $\mathbf{p}(t) \in \mathbb{R}^d$ , and  $\mathbf{J}$  is the  $2d \times 2d$  skew-symmetric matrix defined as:

$$\mathbf{J} = \begin{pmatrix} \mathbf{0}_{d \times d} & \mathbf{I}_{d \times d} \\ -\mathbf{I}_{d \times d} & \mathbf{0}_{d \times d} \end{pmatrix}.$$

The Hamiltonian  $H(z)$  represents the total energy of the molecular system, and is typically ‘separable’ meaning that it can be written as:

$$H(z) = K(\mathbf{p}) + U(\mathbf{q}), \quad z = (\mathbf{q}, \mathbf{p}),$$

where  $K(\mathbf{p})$  and  $U(\mathbf{q})$  are the kinetic and potential energy functions, respectively [81]. In MD, the kinetic energy function is a positive definite quadratic form, and the potential energy function involves

‘fudge factors’ determined from experimental or quantum mechanical studies of pieces of the molecular system of interest [40]. The accuracy of the resulting energy function must be systematically verified by comparing MD simulation data to experimental data [82]. The flow that (1) determines has the following structure:

(S1) volume-preserving (since the vector-field in (1) is divergenceless); and,

(S2) energy-preserving (since  $\mathbf{J}$  is skew-symmetric & constant).

Explicit *symplectic integrators* – like the Verlet scheme – exploit these properties to obtain long-time stable schemes for Hamilton’s equations [83,84].

### 2.2. Governing Stochastic Dynamics

In order to mimic experimental conditions, (1) is often coupled to a bath that puts the system at constant temperature and/or pressure. The standard way to do this is to assume that the system with bath is governed by a stochastic ordinary differential equation (SDE) of the type:

$$d\mathbf{Y}(t) = \underbrace{\mathbf{A}(\mathbf{Y}(t))dt}_{\text{deterministic drift}} + \underbrace{(\text{div } \mathbf{D})(\mathbf{Y}(t))dt + \sqrt{2kT}\mathbf{B}(\mathbf{Y}(t))d\mathbf{W}(t)}_{\text{heat bath}} \tag{2}$$

Here, we have introduced the following notation.

$\mathbf{Y}(t) \in \mathbb{R}^n$	state of the (extended) system
$\mathbf{A}(\mathbf{x}) \in \mathbb{R}^n$	deterministic drift vector field
$\mathbf{B}(\mathbf{x}) \in \mathbb{R}^{n \times n}$	noise-coefficient matrix
$\mathbf{D}(\mathbf{x}) \in \mathbb{R}^{n \times n}$	diffusion matrix
$\mathbf{W}(t) \in \mathbb{R}^n$	$n$ -dimensional Brownian motion
$kT$	temperature factor

The  $n \times n$  *diffusion matrix*  $\mathbf{D}(\mathbf{x})$  is defined in terms of the noise coefficient matrix  $\mathbf{B}(\mathbf{x})$  as:

$$\mathbf{D}(\mathbf{x}) \stackrel{\text{def}}{=} kT\mathbf{B}(\mathbf{x})\mathbf{B}(\mathbf{x})^T, \text{ for all } \mathbf{x} \in \mathbb{R}^n, \tag{3}$$

where  $\mathbf{B}(\mathbf{x})^T$  denotes the transpose of the real matrix  $\mathbf{B}(\mathbf{x})$ . The diffusion matrix is symmetric and nonnegative definite. Depending on the particular bath that is used, the dimension  $n$  of  $\mathbf{Y}(t)$  in (2) is related to the dimension  $2d$  of  $\mathbf{z}(t)$  in (1) by the inequality:  $n \geq 2d$ . For example, in Nosé-Hoover Langevin dynamics a single bath degree of freedom is added to (1) so that  $n = 2d + 1$ , while in Langevin dynamics the effect of the bath is modeled by added friction and Brownian forces that keep  $n = 2d$ . Throughout this work, MD simulation refers to time integration of (2) from a random initial condition.

The equations (2) generate a stochastic process  $\mathbf{Y}(t)$  that is a *Markov diffusion* process. We assume that this diffusion process admits a *stationary* distribution  $\mu(d\mathbf{x})$ , i.e., a probability distribution preserved by the dynamics [85,86]. We denote by  $\nu(\mathbf{x})$  the density of this distribution. Even though the diffusion matrix (3) is not necessarily positive definite, one can use *Hörmander’s condition* to prove that the

process  $\mathbf{Y}(t)$  is an ergodic process with a unique stationary distribution [87,88]. By the ergodic theorem, it then follows that:

$$\frac{1}{T} \int_0^T f(\mathbf{Y}(t)) dt \rightarrow \int_{\mathbb{R}^n} f(\mathbf{x}) \nu(\mathbf{x}) d\mathbf{x} , \text{ as } T \rightarrow \infty, \quad (4)$$

where  $f(\mathbf{x})$  is a suitable test function.

The evolution of the probability density of the law of  $\mathbf{Y}(t)$  at time  $t$ ,  $\rho(t, \mathbf{x})$ , satisfies the Fokker-Planck equation:

$$-\frac{\partial \rho}{\partial t} + L\rho = 0 , \quad (5)$$

where  $\rho(0, \cdot)$  is the density of the initial distribution  $\mathbf{Y}(0) \sim \rho(0, \cdot)$ , and  $\mathcal{L}$  is defined as the following second-order partial differential operator:

$$(Lf)(\mathbf{x}) \stackrel{\text{def}}{=} \text{div}(\text{div}(\mathbf{D}(\mathbf{x})f(\mathbf{x})) - \mathbf{A}(\mathbf{x})f(\mathbf{x})) .$$

Since  $\mu(d\mathbf{x}) = \nu(\mathbf{x})d\mathbf{x}$  is a stationary distribution of  $\mathbf{Y}(t)$ , the probability density  $\nu(\mathbf{x})$  is a steady-state solution of (5):

$$(L\nu)(\mathbf{x}) = 0 . \quad (6)$$

Define the *probability current* as the vector field:

$$\mathbf{j}(\mathbf{x}) \stackrel{\text{def}}{=} \text{div}(\mathbf{D}(\mathbf{x})\nu(\mathbf{x})) - \mathbf{A}(\mathbf{x})\nu(\mathbf{x}) \quad (7)$$

The stationarity condition (6) implies that  $\mathbf{j}(\mathbf{x})$  is divergenceless. In the zero-current case, the diffusion process  $\mathbf{Y}(t)$  is *reversible* and the stationary density  $\nu(\mathbf{x})$  is called the equilibrium probability density of the diffusion [89].

In this case, the operator  $L$  is self-adjoint, in the sense that:

$$\langle Lf, g \rangle_\nu = \langle f, Lg \rangle_\nu \quad \text{for all suitable test functions } f, g , \quad (8)$$

where  $\langle \cdot, \cdot \rangle_\nu$  denotes an  $L^2$  inner product weighted by the density  $\nu(x)$ . This property implies that the diffusion is  $\nu$ -symmetric [90]:

$$\nu(\mathbf{x})p_t(\mathbf{x}, \mathbf{y}) = \nu(\mathbf{y})p_t(\mathbf{y}, \mathbf{x}) \quad \text{for all } t > 0 , \quad (9)$$

where  $p_t(\mathbf{x}, \mathbf{y})$  denotes the transition probability density of  $\mathbf{Y}(t)$ . Indeed (8) is simply an infinitesimal version of (9), which is referred to as the detailed balance condition. In the self-adjoint case, the drift is uniquely determined by the diffusion matrix and the stationary density  $\nu(\mathbf{x})$ :

$$\mathbf{j}(\mathbf{x}) = \mathbf{0} \implies \mathbf{A}(\mathbf{x}) = \frac{1}{\nu(\mathbf{x})} \text{div}(\mathbf{D}(\mathbf{x})\nu(\mathbf{x})) .$$

Long-time stable explicit schemes adapted to this structure have been recently developed [91].

### 2.3. Splitting Approach to MD Simulation

We are now in position to explain our approach to deriving a long-time stable scheme for (2). Crucial to our approach is that in MD simulation we usually have a formula for a function proportional to the stationary density  $\nu(\mathbf{x})$ . Following [92], we can split (2) into:

$$d\mathbf{Y} = -\mathbf{D}(\mathbf{Y})\nabla H_\nu(\mathbf{Y})dt + \text{div } \mathbf{D}(\mathbf{Y})dt + \sqrt{2kT}B(\mathbf{Y})dW \quad (10)$$

$$\dot{\mathbf{Y}} = \mathbf{A}(\mathbf{Y}) + \mathbf{D}(\mathbf{Y})\nabla H_\nu(\mathbf{Y}) \quad (11)$$

where we have introduced  $H_\nu(\mathbf{x}) = -(\log \nu)(\mathbf{x})$ . An *exact splitting method* preserves  $\mu(d\mathbf{x})$ . It is formed by taking the exact solution (in law) of (10) in composition with the exact flow of (11). The process produced by (10) is self-adjoint with respect to  $\nu(\mathbf{x})$ . Moreover, stationarity of  $\nu(\mathbf{x})$  implies that the flow of the ODE (11) preserves it. Since each step is preservative, their composition is too.

In place of the exact splitting, a Metropolis integrator can be used for (10) [91], and a measure-preserving scheme can be designed to solve the ODE [2,93]. In [91], explicit schemes are introduced for (10) that, for the first time: (i) sample the exact equilibrium probability density of the SDE when this density exists (i.e., whenever  $\nu(\mathbf{x})$  is normalizable); (ii) generates a weakly accurate approximation to the solution of (2) at constant  $kT$ ; (iii) acquire higher order accuracy in the small noise limit,  $kT \rightarrow 0$ ; and, (iv) avoid computing the divergence of the diffusion. Compared to the methods in [2], the main novelty of these schemes stems from (iii) and (iv). The resulting explicit splitting method is accurate, since it is an additive splitting of (2); and typically ergodic when the continuous process is ergodic [2].

This type of splitting of (2) is quite natural and has been used before in: MD [77,94], dissipative particle dynamics [95,96], and simulation of inertial particles [97]. Other related schemes for (2) include Brünger-Brooks-Karplus (BBK) [69], van Gunsteren and Berendsen (vGB) [98], the Langevin-Impulse (LI) methods [74], and quasi-symplectic integrators [75]. The long-time statistical properties of this splitting was quantified in the context of globally Lipschitz potential forces in [92]. However, for general MD force fields, none of these explicit integrators are stable. Our framework to stabilize explicit MD integrators is the Metropolis-Hastings algorithm.

### 2.4. Metropolis-Hastings algorithm

A Metropolis-Hastings method is a Monte-Carlo method for producing samples from a probability distribution, given a formula for a function proportional to its density [49,50]. The algorithm consists of two sub-steps: firstly, a proposal move is generated according to a transition density  $g(\mathbf{x}, \mathbf{y})$ ; and second, this proposal move is accepted or rejected with a probability:

$$\alpha(\mathbf{x}, \mathbf{y}) = 1 \wedge \frac{g(\mathbf{y}, \mathbf{x})\nu(\mathbf{y})}{g(\mathbf{x}, \mathbf{y})\nu(\mathbf{x})}. \quad (12)$$

Standard results on Metropolis-Hastings methods can be used to classify this algorithm as ergodic [87, 99,100].

### 3. Algorithmic Introduction to MD Integrators

We now focus our discussion on Langevin dynamics of a system of  $N$  atoms. Denote by  $m_j > 0$  and  $\mathbf{q}_j$  the mass and position of the  $j$ th atom, respectively. The governing Langevin equation is given by:

$$\begin{cases} \dot{\mathbf{q}}_j(t) = m_j^{-1} \mathbf{p}_j(t), \\ d\mathbf{p}_j(t) = -\frac{\partial U}{\partial \mathbf{q}_j}(\mathbf{q}(t))dt - \gamma \mathbf{p}_j(t)dt + \sqrt{2kT\gamma m_j} d\mathbf{w}_j, \end{cases} \quad j = 1, \dots, N, \quad (13)$$

where  $\mathbf{q} = (\mathbf{q}_1, \dots, \mathbf{q}_N)$  and  $\mathbf{p} = (\mathbf{p}_1, \dots, \mathbf{p}_N)$  denote the positions and momenta of the particles, and  $\mathbf{w}_j$  are independent Brownian motions. In Langevin dynamics, positions are differentiable, and due to the irregularity of the Brownian force, momenta are just continuous but not differentiable. The last two terms in the second equation represent the effect of the bath. The bath-free dynamics is a Hamiltonian system with:

$$H(\mathbf{q}, \mathbf{p}) = \sum_{j=1}^N \frac{1}{2m_j} |\mathbf{p}_j|^2 + U(\mathbf{q}).$$

The stationary distribution of the Langevin process has the following density:

$$\nu(\mathbf{q}, \mathbf{p}) = Z^{-1} \exp\left(-\frac{1}{kT} H(\mathbf{q}, \mathbf{p})\right), \quad Z = \int \exp\left(-\frac{1}{kT} H(\mathbf{q}, \mathbf{p})\right) d\mathbf{q} d\mathbf{p}. \quad (14)$$

The Langevin equation (13) can be put in the form of (2) by letting  $\mathbf{x} = (\mathbf{q}, \mathbf{p})$ ,

$$\mathbf{A}(\mathbf{x}) = \begin{pmatrix} \mathbf{m}^{-1} \mathbf{p} \\ -\nabla U(\mathbf{q}) - \gamma \mathbf{p} \end{pmatrix}, \quad \mathbf{B} = \sqrt{\gamma} \begin{pmatrix} \mathbf{0} & \mathbf{0} \\ \mathbf{0} & \mathbf{m}^{1/2} \end{pmatrix}, \quad \text{and } \mathbf{W} = (\mathbf{w}_1, \dots, \mathbf{w}_N), \quad (15)$$

where  $\mathbf{m} = \text{diag}(m_1, \dots, m_N)$ . The splitting approach discussed in §2 applied to Langevin dynamics (13) leads to the following special cases of (10) and (11):

$$\begin{cases} d\mathbf{p}(t) = -\gamma \mathbf{p}(t)dt + \sqrt{2kT\gamma} \mathbf{m}^{1/2} d\mathbf{W}, \end{cases} \quad (16)$$

$$\begin{cases} \dot{\mathbf{q}}(t) = \mathbf{m}^{-1} \mathbf{p}(t), \\ \dot{\mathbf{p}}(t) = -\nabla U(\mathbf{q}(t)). \end{cases} \quad (17)$$

Notice that (16) is a linear SDE that can be exactly solved [101, See Chapter 5]. We will use a Verlet integrator for (17) that preserves volume and represents the energy to third-order accuracy per step. Since the Verlet integrator does not exactly preserve energy, the composition of the two schemes does not preserve the stationary distribution with density (14). As a consequence of this discretization error, this scheme may either not detect properly features of the potential energy, which leads to unnoticed but large errors in dynamic quantities such as the mean first passage time, or may mishandle soft or hard-core potentials, which leads to numerical instabilities; see the numerical examples in [91]. These numerical artifacts motivate adding a Metropolis accept/refusal sub-step to the integrator. The *corrected* MD integrator follows.

**Algorithm 3.1** (Analysis-based MD Integrator). Given the current state  $(\mathbf{Q}_0, \mathbf{P}_0)$  at time  $t$  the algorithm proposes a position  $(\mathbf{Q}_1^*, \mathbf{P}_1^*)$  at time  $t + h$  for some time-step  $h > 0$  via

$$\begin{cases} \mathbf{P}_{1/2} = \mathbf{P}_0 - \frac{h}{2} \nabla U(\mathbf{Q}_0) \\ \mathbf{Q}_1^* = \mathbf{Q}_0 + h \mathbf{P}_{1/2} \\ \mathbf{P}_1^* = \mathbf{P}_{1/2} - \frac{h}{2} \nabla U(\mathbf{Q}_1^*) \end{cases} \quad (\text{Step 1})$$

The ‘proposal move’  $(\mathbf{Q}_1^*, \mathbf{P}_1^*)$  is then accepted or rejected:

$$\begin{pmatrix} \tilde{\mathbf{Q}}_1 \\ \tilde{\mathbf{P}}_1 \end{pmatrix} = x \begin{pmatrix} \mathbf{Q}_1^* \\ \mathbf{P}_1^* \end{pmatrix} + (1 - x) \begin{pmatrix} \mathbf{Q}_0 \\ -\mathbf{P}_0 \end{pmatrix}, \quad (\text{Step 2})$$

where  $x$  is a Bernoulli random variable with parameter  $\alpha$ , i.e., it takes value 1 with probability  $\alpha$  and value 0 with probability  $1 - \alpha$ . The acceptance probability is defined as:

$$\alpha = 1 \wedge \exp\left(-\frac{1}{kT}(H(\mathbf{Q}_1^*, \mathbf{P}_1^*) - H(\mathbf{Q}_0, \mathbf{P}_0))\right). \quad (18)$$

The actual update of the system is taken to be:

$$\begin{pmatrix} \mathbf{Q}_1 \\ \mathbf{P}_1 \end{pmatrix} = \begin{pmatrix} \tilde{\mathbf{Q}}_1 \\ \exp(-\gamma h) \tilde{\mathbf{P}}_1 + \sqrt{1 - \exp(-2\gamma h)} \mathbf{m}^{1/2} \boldsymbol{\xi} \end{pmatrix}. \quad (\text{Step 3})$$

Here  $\boldsymbol{\xi} \in \mathbb{R}^n$  denotes a Gaussian random vector with mean zero and covariance  $\mathbb{E}(\boldsymbol{\xi}_i \boldsymbol{\xi}_j) = kT \delta_{ij}$ .

Notice that the momentum gets flipped if a move is rejected in (Step 2). This momentum flip is necessary in order to guarantee that the algorithm samples the correct stationary distribution [48], but results in a  $O(1)$  error in dynamics. To compute dynamics not only must a long trajectory be stably produced with the right stationary distribution, but the approximation must also accurately represent the system’s dynamics over the time interval of interest. Unlike sampling algorithms, high acceptance rates are needed to ensure that the time lag between successive rejections is frequently long enough to capture the desired dynamics. Since the acceptance rate in (18) is related to how well the Verlet step preserves energy after a single step, this rejection rate is  $O(h^3)$ . Thus, in practice we find that the time-step required to obtain a 99.9% acceptance rate is often automatically satisfied with a time-step that sufficiently resolves the desired dynamics. Each step of this algorithm requires: evaluating the atomic force field once in the third equation of (Step 1), generating a Bernoulli random variable with parameter  $\alpha$  in (Step 2), and generating an  $n$ -dimensional Gaussian vector in (Step 3). Since (Step 3) is the exact solution of (10), we stress that (Step 2) in Algorithm 3.1 is all that is really needed in most MD integration schemes to ensure that the integrator preserves the correct stationary density (14).

Listing 1 translates Algorithm 3.1 into the MATLAB language. Intrinsicly defined MATLAB functions appear in boldface. The algorithm uses MATLAB’s built in random number generators to carry out (Step 2) and (Step 3). In particular, the Bernoulli random variable  $x$  in (Step 2) is generated in *Line*



15, and the Gaussian vector in (Step 3) is generated on *Line 24*. In addition to updating the positions and momenta of the system, the program also stores the previous value of the potential energy and force, so that the force and potential energy is evaluated just once in *Line 12* per simulation step. This evaluation calls a MEX function which inputs the current position of the molecular system and outputs the force field and potential energy at that position. We use a MEX function because the atomistic force-field evaluation cannot be easily vectorized, and is by far, the most computationally demanding step in MD. The `PreProcessing` script file called in *Line 2* defines the physical and numerical parameters, sets the initial condition, and allocates space for storing simulation data. Sample averages are updated as new points on the trajectory are produced in the `UpdateSampleAverages` script file invoked in *Line 30*. Finally, the outputs produced by the algorithm are handled by the `PostProcessing` script file in *Line 34*.

Let us consider a concrete example: a Lennard-Jones fluid that consists of  $N$  identical atoms [4–6]. The configuration space of this system is a fixed cubic box with periodic boundary conditions. The distance between the  $i$ th and  $j$ th particle is defined according to the *minimum image convention*, which states that the distance between  $\mathbf{q}_i$  and  $\mathbf{q}_j$  in a cubic box of length  $\ell$  is:

$$d_{MD}(\mathbf{q}_i, \mathbf{q}_j) \stackrel{\text{def}}{=} |(\mathbf{q}_i - \mathbf{q}_j) - \ell \lfloor (\mathbf{q}_i - \mathbf{q}_j) / \ell \rfloor| . \quad (19)$$

where  $\lfloor \cdot \rfloor$  is the nearest integer function. In terms of this distance, the total potential energy is a sum over all pairs:

$$U(\mathbf{q}) = \sum_{i=1}^{n-1} \sum_{j=i+1}^n U_{LJ}(d_{MD}(\mathbf{q}_i, \mathbf{q}_j)) , \quad (20)$$

where  $U_{LJ}(r)$  is the following truncated Lennard-Jones potential function:

$$U_{LJ}(r) = \begin{cases} f(r) - f(r_c) & r < r_c , \\ 0 & \text{otherwise} . \end{cases} \quad (21)$$

Here,  $f(r) = 4(1/r^{12} - 1/r^6)$  and  $r_c$  is the cutoff radius which is bounded above by the size of the simulation box; and we have used dimensionless units to describe this system, where energy is rescaled by the depth of the Lennard-Jones potential energy and length by the point where the potential energy is zero. The error introduced by the truncation in (21) is proportional to the density of the molecular system and can be made arbitrarily small by selecting the cutoff distance sufficiently large. Unless a neighbor and/or cell list is employed, a direct evaluation of the potential force  $\nabla U(\mathbf{q})$  scales like  $O(N^2)$ , and typically dominates the total computational cost [76]. Since the molecular system we consider will have just a few hundred atoms, we found that there is no advantage to using a fast force–field evaluation, and thus `ForceFieldmex` evaluates the force and energy using a sum over all particle pairs.

Listing 2 shows the `PreProcessing` script which sets the parameters provided in Table 1 and constructs the initial condition, where the  $N$  atoms are assumed to be at rest and on the sites of an FCC lattice. The command `rng(123)` on *Line 3* sets the seed of the random number generator functions `RAND` and `RANDN`. The acceptance rates at every step and the velocity autocorrelation are updated in the `UpdateSampleAverages` script shown in Listing 3. The mean acceptance rate which

---

**Listing 1.** Analysis-Based MD Integrator: MDintegrator.m
 

---

```

1
2 PreProcessing;
3
4 for i = 1:Ns
5
6     %--- Step 1 --- Velocity Verlet Proposal
7
8     Ppt5=P0+0.5*h*F0;
9     Q1star=Q0+h*Ppt5;
10    [F1star,U1star]=ForceFieldmex(Q1star,Nm,rcut2,ell);
11    P1star=Ppt5+0.5*h*F1star;
12
13    %--- Step 2 --- Accept or Refuse Step
14
15    x=(rand<exp(-(0.5*P1star'*P1star-0.5*P0'*P0+U1star-U0)/kT));
16
17    tildeP1=x*P1star-(1-x)*P0;
18    tildeQ1=x*Q1star+(1-x)*Q0;
19    F1=x*F1star+(1-x)*F0; U1=x*U1star+(1-x)*U0;
20
21    %--- Step 3 --- Heat Bath Step
22
23    Q1=tildeQ1;
24    P1=f1*tildeP1+f2*randn(3*Nm,1);
25
26    %--- iterate
27
28    Q0=Q1; P0=P1; F0=F1; U0=U1;
29
30    UpdateSampleAverages;
31
32 end
33
34 PostProcessing;

```

---

is outputted in the script `PostProcessing` shown in Listing 4 must be high enough to ensure that the dynamics is accurately represented. To compute the autocorrelation of an observable over a time interval of length  $T$ , the value of that observable along the entire trajectory is not needed. In fact, all that is really needed are the values of this observable along a piece of trajectory over the moving time-window  $[t_i, t_i + T]$  where  $t_i = i \times h$ . This storage space is allocated in `PreProcessing` and is updated in `UpdateSampleAverages`. More precisely, since we define  $N_a = \lceil T/h \rceil + 1$  in the `PreProcessing` script, the molecular velocities are stored in the `pivot` array from  $i - N_a$  to  $i$ , where  $i$  is the index of the current position. Notice that velocity autocorrelations are not computed until after the index  $i$  exceeds  $10^4$ . This *equilibration time* removes some of the statistical bias that may arise from using a non-random initial condition. Short-time trajectories of this molecular system are plotted in Figure 2. This figure shows that the particle motions are more localized at higher densities. Using the parameters provided in Table 1, we compute velocity autocorrelations for a range of density values in Figure 3. Since the heat bath parameter is set to a small value, these figures are in agreement with those obtained by simulating the molecular system with no heat bath in Figure 5.2 of [6].

**Figure 2. Atomic Trajectories in Simulation Box.** Plot of individual atomic trajectories from an initial condition where atoms are placed on the sites of an FCC lattice and at rest. The trajectory is computed using the numerical and physical parameters indicated in Table 1, with the exception of the # of steps which is set equal to  $N_s = 1000$ . At the lower densities the particle trajectories are more diffusive and less localized.

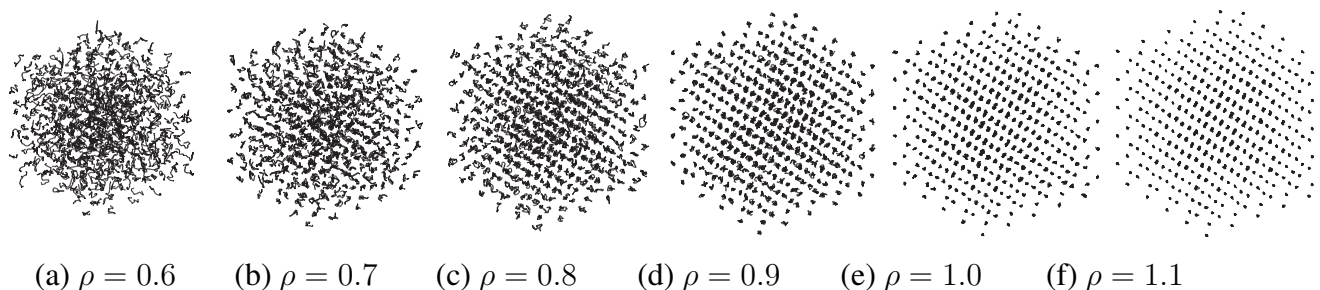


**Table 1. Simulation Parameters.**

Parameter	Description	Value
<i>Physical Parameters</i>		
$\rho$	density	{0.6, 0.7, 0.8, 0.9, 1.0, 1.1}
$kT$	temperature	0.5
$\gamma$	heat bath parameter	0.01
$N_m$	# of molecules	512
$T$	time-span for autocorrelation	2
<i>Numerical Parameters</i>		
$h$	time-step	0.005
$N_s$	# of simulation steps	$10^5$
$r_c$	LJ cutoff radius	$2^{1/6}$

---

**Listing 2.** Analysis-Based MD Integrator: PreProcessing.m
 

---

```

1 %--- seed random # generator
2
3 rng(123);
4
5 %--- physical parameters
6
7 rho=0.6;           % density
8 kT=0.5;           % temperature factor
9 gama=0.1;         % heat bath parameter
10 Nm=500;           % # of molecules
11 T=2.0;            % time span for velocity correlation
12 ell=(Nm/rho)^(1/3); % length of cubic box
13
14 %--- simulation parameters
15
16 h=0.005;          % time-step size
17 Ns=1e3;           % # of steps
18 rcut = 2.0^(1/6); % cutoff radius
19 rcut2 = rcut*rcut;
20
21 f1=exp(-gama*h); f2=sqrt((1.0-exp(-2.0*gama*h))*kT);
22
23 %--- initial condition
24
25 A=fcclattice(Nm,ell);
26 Q0=reshape(A, [3*Nm 1]); % atoms on an fcc lattice
27 P0=zeros(3*Nm,1); % atoms at rest
28
29 %--- initialize statistics
30
31 NA=ceil(T/h)+1; % preallocate space for
32 acf=zeros(NA,1); % online correlation computation
33 varacf=zeros(NA,1);
34 pivot=zeros(NA,3*Nm);
35 nacf=zeros(NA,1);
36
37 AP=zeros(Ns,1); % vector of acceptance probabilities
38
39 [F0,U0]=ForceFieldmex(Q0,Nm,rcut2,ell); % initial force & energy

```

---

**Listing 3.** Analysis-Based MD Integrator: UpdateSampleAverages.m

---

```

1 %--- store acceptance probability
2
3 AP(i)=x;
4
5 %--- update correlation function
6
7 if (i>1e4)
8
9     pp=mod(i-1,NA)+1;
10    pivot(pp,:)=P0;
11
12    for j=1:min(i,NA)
13        nacf(j)=nacf(j)+1;
14        mui=acf(j);
15        vari=varacf(j);
16        n_samples=nacf(j);
17        xip1=pivot(mod(pp-j,NA)+1,:)*pivot(pp,:)/(3.0*Nm);
18        acf(j)=mui+(xip1-mui)/n_samples;
19        varacf(j)=(n_samples-1)*vari+...
20                (xip1-mui)*(xip1-acf(j))/n_samples;
21    end
22
23 end

```

---

**Listing 4.** Analysis-Based MD Integrator: PostProcessing.m

---

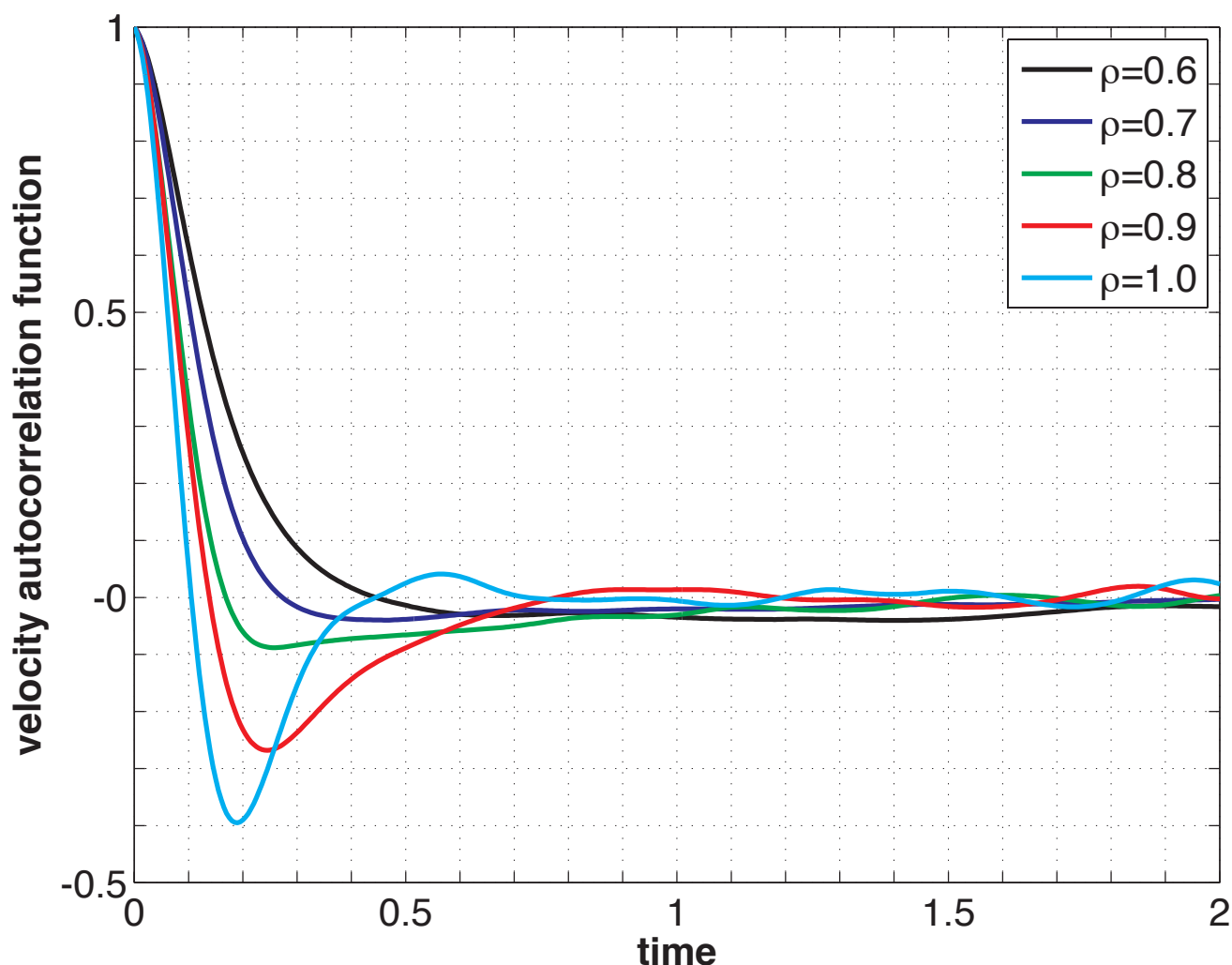
```

1 %--- output results
2
3 disp(['h=' num2str(h) ', <AP>=' num2str(mean(AP))]);
4
5 figure(2); clf; hold on; tt=0:h:T;
6 errorbar(tt,acf,1.96*sqrt(varacf)./sqrt(nacf));
7
8 save('VelocityAutocorrelation.mat', 'tt', 'acf', 'varacf');

```

---

**Figure 3. Soft-sphere Velocity Autocorrelation Functions.** A reproduction of Figure 5.2 of [6] using Langevin dynamics with heat bath parameter  $\gamma = 0.01$ . The remaining parameters are set equal to those provided in Table 1. The negative correlations at higher densities are consistent with what has been found in the literature [9,11].



#### 4. Potential Pitfalls in High Dimension & Tricks for Mitigation

For high dimensional systems (think  $N > 10^3$  atoms), calculating the force-field at every step is the main computational cost of MD simulation. These force fields involve: bonded interactions, and non-bonded Lennard-Jones & electrostatic interactions. The calculation of bonded interactions is straightforward to vectorize and scales like  $O(N)$ . In addition, Lennard-Jones forces rapidly decay with interatomic distance. To a good approximation, every atom interacts only with neighbors within a sufficiently large ball. By using data structures like neighbor lists and cell linked-lists, these interactions can be calculated in  $O(N)$  steps, and therefore, the Lennard-Jones interactions can be calculated in  $O(N)$  steps [76]. On the other hand, the electrostatic energy between particles decays like  $1/r$  where  $r$  denotes an interbead distance which leads to long-range interactions between atoms. Unlike Lennard-Jones interaction, this interaction cannot be cutoff without introducing large errors. In this case, one can

use sophisticated analysis-based techniques like the fast multipole method to rigorously handle such interactions in  $\mathcal{O}(N)$  steps [35,72].

However, the effect of these ‘mathematical tricks’ for fast calculation of the force field can become muted if the time-step requirement for stability or accuracy becomes more severe in high dimension. This can happen in the Metropolis integrator, if the acceptance probability in (Step 2) of Algorithm 3.1 deteriorates in high dimension. The scaling of Metropolis algorithms has been quantified for the random walk Metropolis, hybrid Monte-Carlo, and MALA algorithms [102–106]. Since the acceptance probability is a function of an extensive quantity, the acceptance rate can artificially deteriorate with increasing system size unless the time-step is reduced. Because high acceptance rates are required to maintain dynamic accuracy, the dependence of the time-step on system size limits the application of Metropolized schemes to large-scale systems. Fortunately, this scalability issue can often be resolved by using local rather than global proposal moves because the change in energy induced by a local move is typically an intensive quantity. For molecular dynamics calculations, this approach was pursued in [3]. Using dynamically consistent local moves (a so-called J-splitting [107]), it was shown that in certain situations a scalable Metropolis integrator can be designed; however, the extent to which this strategy remedies the issue of high rejection rate in high dimension is not clear at this point, and should be tested in applications.

## 5. Conclusion

This paper provided a step-by-step algorithmic introduction to new *analysis-based* MD integrators for MD simulation. These algorithms are long-time stable and finite-time accurate for MD simulation. A MATLAB implementation of the algorithm was provided, and used to compute the velocity autocorrelation of a sea of Lennard–Jones particles at various densities between the solid and liquid phases. The paper did not review the theory of Metropolis integrators which is discussed elsewhere [2,3]. We conclude by mentioning two directions for future development.

- The compatibility of the Metropolis integrator with a fast multipole method for handling the electrostatic effects has not been investigated. This loose end is indicated by the question mark appearing towards the right end of the timeline in Figure 1, which points out that an  $\mathcal{O}(N)$  Metropolis integrator is currently unavailable.
- Another issue is the development of second-order Metropolis integrators for (13) which might permit larger time-steps. The ‘quasi-symplectic’ second-order Langevin integrators introduced in [77] would be a natural starting point for designing proposal moves that would lead to second-order Metropolis integrators.

## Acknowledgements

The research that led to this paper was made possible by NSF grant DMS-1212058.

## Conflict of Interest

The authors declare no conflict of interest.

## References

1. MATLAB. *Version 8.0.0 (R2012b)*; The MathWorks Inc.: Natick, Massachusetts, 2012.
2. Bou-Rabee, N.; Vanden-Eijnden, E. Pathwise accuracy and ergodicity of Metropolized Integrators for SDEs. *Comm Pure and Appl Math* **2010**, *63*, 655–696.
3. Bou-Rabee, N.; Vanden-Eijnden, E. A patch that imparts unconditional stability to explicit integrators for Langevin-like equations. *J Comput Phys* **2012**, *231*, 2565–2580.
4. Allen, M.P.; Tildesley, D.J. *Computer Simulation of Liquids*; Clarendon Press, 1987.
5. Frenkel, D.; Smit, B. *Understanding Molecular Simulation: From algorithms to Applications, Second Edition*; Academic Press, 2002.
6. Rapaport, D.C. *The art of molecular dynamics simulation*; Cambridge university press, 2004.
7. Tuckerman, M. *Statistical Mechanics and Molecular Simulations*; Oxford University Press, 2008.
8. Schlick, T. *Molecular modeling and simulation: an interdisciplinary guide*; Vol. 21, Springer, 2010.
9. Rahman, A. Correlations in the motion of atoms in liquid argon. *Phys Rev* **1964**, *136*, A405.
10. Verlet, L. Computer “experiments” on Classical Fluids. I. Thermodynamical properties of Lennard-Jones molecules. *Phys Rev* **1967**, *159*, 98–103.
11. Alder, B.J.; Wainwright, T.E. Velocity autocorrelations for hard spheres. *Phys Rev Lett* **1967**, *18*, 988.
12. Alder, B.J.; Gass, D.M.; Wainwright, T.E. Studies in Molecular Dynamics. VIII. The Transport Coefficients for a Hard-Sphere Fluid. *J Chem Phys* **1970**, *53*, 3813.
13. Harp, G.D.; Berne, B.J. Time-correlation functions, memory functions, and molecular dynamics. *Phys Rev A* **1970**, *2*, 975.
14. Rahman, A.; Stillinger, F.H. Molecular dynamics study of liquid water. *J Chem Phys* **1971**, *55*, 3336.
15. Stillinger, F.H.; Rahman, A. Improved simulation of liquid water by molecular dynamics. *J Chem Phys* **1974**, *60*, 1545.
16. Stillinger, F.H. Water revisited. *Science* **1980**, *209*, 451–457.
17. McCammon, A.J.; Gelin, B.R.; Karplus, M. Dynamics of folded proteins. *Nature* **1977**, *267*, 585–590.
18. Van Gunsteren, W.F.; Berendsen, H.J.C. Algorithms for macromolecular dynamics and constraint dynamics. *Mol Phys* **1977**, *34*, 1311–1327.
19. McCammon, J.A.; Karplus, M. Simulation of protein dynamics. *Annual Review of Physical Chemistry* **1980**, *31*, 29–45.
20. Van Gunsteren, W.F.; Karplus, M. Protein dynamics in solution and in a crystalline environment: a molecular dynamics study. *Biochemistry* **1982**, *21*, 2259–2274.
21. Karplus, M.; McCammon, A.J. Dynamics of proteins: elements and function. *Annual review of biochemistry* **1983**, *52*, 263–300.



22. van Gunsteren, W.F.; Berendsen, H.J.C. Computer simulation of molecular dynamics: Methodology, applications, and perspectives in chemistry. *Angewandte Chemie International Edition in English* **1990**, *29*, 992–1023.
23. Karplus, M.; McCammon, A.J. Molecular dynamics simulations of biomolecules. *Nature Structural & Molecular Biology* **2002**, *9*, 646–652.
24. Case, D.A. Molecular dynamics and NMR spin relaxation in proteins. *Accounts of chemical research* **2002**, *35*, 325–331.
25. Adcock, A.S.; McCammon, A.J. Molecular dynamics: survey of methods for simulating the activity of proteins. *Chemical reviews* **2006**, *106*, 1589–1615.
26. van Gunsteren, W.F.; Dolenc, J.; Mark, A.E. Molecular simulation as an aid to experimentalists. *Current opinion in structural biology* **2008**, *18*, 149–153.
27. Kapral, R.; Ciccotti, G. Molecular dynamics: an account of its evolution. *Theory and applications of computational chemistry: the first forty years* **2005**, p. 425.
28. Scheraga, H.A.; Khalili, M.; Liwo, A. Protein-folding dynamics: overview of molecular simulation techniques. *Annu Rev Phys Chem* **2007**, *58*, 57–83.
29. Dror, R.O.; Dirks, R.M.; Grossman, J.P.; Xu, H.; Shaw, D.E. Biomolecular simulation: a computational microscope for molecular biology. *Annual Review of Biophysics* **2012**, *41*, 429–452.
30. Lane, T.J.; Shukla, D.; Beauchamp, K.A.; Pande, V.S. To milliseconds and beyond: challenges in the simulation of protein folding. *Current opinion in structural biology* **2012**.
31. Nielsen, S.O.; Lopez, C.F.; Srinivas, G.; Klein, M.L. Coarse grain models and the computer simulation of soft materials. *Journal of Physics: Condensed Matter* **2004**, *16*, R481.
32. Tozzini, V. Coarse-grained models for proteins. *Current opinion in structural biology* **2005**, *15*, 144–150.
33. Clementi, C. Coarse-grained models of protein folding: toy models or predictive tools? *Current opinion in structural biology* **2008**, *18*, 10–15.
34. Sherwood, P.; Brooks, B.R.; Sansom, M.S.P. Multiscale methods for macromolecular simulations. *Current opinion in structural biology* **2008**, *18*, 630–640.
35. Weinan, E. *Principles of multiscale modeling*; Cambridge University Press, 2011.
36. E, W.; Vanden-Eijnden, E. Metastability, conformation dynamics, and transition pathways in complex systems. In *Multiscale Modelling and Simulation*; Attinger, S.; Koumoutsakos, P., Eds.; Lecture Notes in Computational Science and Engineering, Springer, 2004; pp. 35–68.
37. Vanden-Eijnden, E.; Venturoli, M. Markovian milestoning with Voronoi tessellations. *J Chem Phys* **2009**, *130*, 194101.
38. Vanden-Eijnden, E.; Venturoli, M. Exact rate calculations by trajectory parallelization and twisting. *J Chem Phys* **2009**, *131*, 044120.
39. E, W.; Vanden-Eijnden, E. Transition-Path Theory and Path-Finding Algorithms for the Study of Rare Events. *Annual Review of Physical Chemistry* **2010**, *61*, 391–420.
40. Brooks, B.R.; Brucoleri, R.E.; Olafson, B.D.; Swaminathan, S.; Karplus, M.; others. CHARMM: A program for macromolecular energy, minimization, and dynamics calculations. *J Comp Chem* **1983**, *4*, 187–217.

41. Nelson, M.T.; Humphrey, W.; Gursoy, A.; Dalke, A.; Kalé, L.V.; Skeel, R.D.; Schulten, K. NAMD: a parallel, object-oriented molecular dynamics program. *International Journal of High Performance Computing Applications* **1996**, *10*, 251–268.
42. Scott, W.R.P.; Hünenberger, P.H.; Tironi, I.G.; Mark, A.E.; Billeter, S.R.; Fennen, J.; Torda, A.E.; Huber, T.; Krüger, P.; van Gunsteren, W.F. The GROMOS biomolecular simulation program package. *J Phys Chem A* **1999**, *103*, 3596–3607.
43. Talay, D. Stochastic Hamiltonian Systems: Exponential Convergence to the Invariant Measure, and Discretization by the Implicit Euler Scheme. *Markov Processes and Related Fields* **2002**, *8*, 1–36.
44. Higham, D.J.; Mao, X.; Stuart, A.M. Strong Convergence of Euler-Type Methods for Nonlinear Stochastic Differential Equations. *IMA J Num Anal* **2002**, *40*, 1041–1063.
45. Milstein, G.N.; Tretyakov, M.V. Numerical Integration of Stochastic Differential Equations with Nonglobally Lipschitz Coefficients. *IMA J Num Anal* **2005**, *43*, 1139–1154.
46. Higham, D.J. Stochastic ordinary differential equations in applied and computational mathematics. *IMA J Appl Math* **2011**, *76*, 449–474.
47. Hutzenthaler, M.; Jentzen, A.; Kloeden, P.E. Strong convergence of an explicit numerical method for SDEs with non-globally Lipschitz continuous coefficients. *Ann Appl Probab* **2012**, *22*, 1611–1641.
48. Akhmatkaya, E.; Bou-Rabee, N.; Reich, S. A Comparison of Generalized Hybrid Monte Carlo Methods with and without Momentum Flip. *J Comput Phys* **2009**, *228*, 2256–2265.
49. Metropolis, N.; Rosenbluth, A.W.; Rosenbluth, M.N.; Teller, A.H.; Teller, E. Equations of State Calculations by Fast Computing Machines. *J Chem Phys* **1953**, *21*, 1087–1092.
50. Hastings, W.K. Monte-Carlo Methods Using Markov Chains and Their Applications. *Biometrika* **1970**, *57*, 97–109.
51. Rossky, P.J.; Doll, J.D.; Friedman, H.L. Brownian dynamics as smart Monte Carlo simulation. *J Chem Phys* **1978**, *69*, 4628.
52. Duane, S.; Kennedy, A.D.; Pendleton, B.J.; Roweth, D. Hybrid Monte-Carlo. *Phys Lett B* **1987**, *195*, 216–222.
53. Horowitz, A.M. A Generalized Guided Monte-Carlo Algorithm. *Phys Lett B* **1991**, *268*, 247–252.
54. Kennedy, A.D.; Pendleton, B. Cost of the generalized hybrid Monte Carlo algorithm for free field theory. *Nucl. Phys. B* **2001**, *607*, 456–510.
55. Liu, J.S. *Monte Carlo Strategies in Scientific Computing*, 2nd ed.; Springer, 2008.
56. Akhmatkaya, E.; Reich, S. GSHMC: An efficient method for molecular simulation. *J Comput Phys* **2008**, *227*, 4937–4954.
57. Lelièvre, T.; Rousset, M.; Stoltz, G. *Free Energy Computations: A Mathematical Perspective*, 1st ed.; Imperial College Press, 2010.
58. The Mathworks Inc.. Introducing MEX-files. [http://www.mathworks.com/help/matlab/matlab\\_external/introducing-mex-files.html](http://www.mathworks.com/help/matlab/matlab_external/introducing-mex-files.html). [Online; accessed 15-July-2013].
59. Levitt, M. Molecular dynamics of native protein: I. computer simulation of trajectories. *Journal of molecular biology* **1983**, *168*, 595–617.

60. Levitt, M.; Sharon, R. Accurate simulation of protein dynamics in solution. *Proceedings of the National Academy of Sciences* **1988**, *85*, 7557–7561.
61. Daggett, V.; Levitt, M. A model of the molten globule state from molecular dynamics simulations. *Proceedings of the National Academy of Sciences* **1992**, *89*, 5142–5146.
62. Li, A.; Daggett, V. Investigation of the solution structure of chymotrypsin inhibitor 2 using molecular dynamics: comparison to X-ray crystallographic and NMR data. *Protein engineering* **1995**, *8*, 1117–1128.
63. Duan, Y.; Kollman, P.A. Pathways to a protein folding intermediate observed in a 1-microsecond simulation in aqueous solution. *Science* **1998**, *282*, 740–744.
64. Freddolino, P.L.; Liu, F.; Gruebele, M.; Schulten, K. Ten-microsecond molecular dynamics simulation of a fast-folding WW domain. *Biophysical journal* **2008**, *94*, 75–77.
65. Shaw, D.E.; Maragakis, P.; Lindorff-Larsen, K.; Piana, S.; Dror, R.O.; Eastwood, M.P.; Bank, J.A.; Jumper, J.M.; Salmon, J.K.; Shan, Y. Atomic-level characterization of the structural dynamics of proteins. *Science* **2010**, *330*, 341–346.
66. Quentrec, B.; Brot, C. New method for searching for neighbors in molecular dynamics computations. *J Comput Phys* **1973**, *13*, 430–432.
67. Ryckaert, J.; Ciccotti, G.; Berendsen, H. Numerical Integration of the Cartesian Equations of Motion of a System with Constraints: Molecular dynamics of n-alkanes. *J Comput Phys* **1977**, *23*, 327–341.
68. Schneider, T.; Stoll, E. Molecular-dynamics study of a three-dimensional one-component model for distortive phase transitions. *Phys Rev B* **1978**, *17*, 1302–1322.
69. Brünger, A.; Brooks, C.L.; Karplus, M. Stochastic Boundary Conditions for Molecular Dynamics Simulations of ST2 Water. *Chem Phys Lett* **1984**, *105*, 495–500.
70. Nosé, S. A Unified Formulation for Constant Temperature Molecular Dynamics Methods. *J Chem Phys* **1984**, *81*, 511.
71. Hoover, W.G. Canonical Dynamics: Equilibrium Phase-Space Distributions. *Phys Rev A* **1985**, *31*, 1695.
72. Greengard, L.; Rokhlin, V. A fast algorithm for particle simulations. *J Comput Phys* **1987**, *73*, 325–348.
73. Tuckerman, M.E.; Berne, B.J.; Martyna, G. Reversible multiple time scale molecular dynamics. *J Chem Phys* **1992**, *97*, 1990–2001.
74. Skeel, R.D.; Izaguirre, J. An Impulse Integrator for Langevin Dynamics. *Mol Phys* **2002**, *100*, 3885–3891.
75. Milstein, G.N.; Tretyakov, M.V. Quasi-symplectic methods for Langevin-type equations. *IMA J Num Anal* **2003**, *23*, 593–626.
76. Yao, Z.; Wang, J.S.; Liu, G.R.; Cheng, M. Improved neighbor list algorithm in molecular simulations using cell decomposition and data sorting method. *Computer physics communications* **2004**, *161*, 27–35.
77. Vanden-Eijnden, E.; Ciccotti, G. Second-order integrators for Langevin equations with holonomic constraints. *Chem Phys Lett* **2006**, *429*, 310–316.

78. Samoletov, A.A.; Chaplain, M.A.; Dettmann, C.P. Thermostats for “Slow” Configurational Modes. *J Stat Phys* **2008**, *128*, 1321–1336.
79. Leimkuhler, B.; Noorizadeh, E.; Theil, F. A Gentle Stochastic Thermostat for Molecular Dynamics. *J Stat Phys* **2009**, *135*, 261–277.
80. Leimkuhler, B.; Reich, S. A Metropolis adjusted Nosé-Hoover Thermostat. *ESAIM: M2AN* **2009**, *43*, 743–755.
81. Marsden, J.; Ratiu, T. *Introduction to Mechanics and Symmetry*; Springer Texts in Applied Mathematics, 1999.
82. van Gunsteren, W.F.; Mark, A.E. Validation of molecular dynamics simulation. *J Chem Phys* **1998**, *108*, 6109.
83. Leimkuhler, B.; Reich, S. *Simulating Hamiltonian Dynamics*; Cambridge Monographs on Applied and Computational Mathematics, Cambridge University Press, 2004.
84. Hairer, E.; Lubich, C.; Wanner, G. *Geometric Numerical Integration*; Springer, 2010.
85. Ikeda, N.; Watanabe, S. *Stochastic Differential Equations and Diffusion Processes*; North-Holland, 1989.
86. Klebaner, F.C. *Introduction to stochastic calculus with applications*; Imperial College Press, 2005.
87. Mengersen, K.L.; Tweedie, R.L. Rates of Convergence of the Hastings and Metropolis Algorithms. *Ann Stat* **1996**, *24*, 101–121.
88. Prato, G.D.; Zabczyk, J. *Ergodicity for Infinite Dimensional Systems*; Cambridge University Press, 1996.
89. Haussman, U.G.; Pardoux, E. Time Reversal for Diffusions. *Annals of Probability* **1986**, *14*, 1188–1205.
90. Kent, J. Time-reversible diffusions. *Adv Appl Prob* **1978**, *10*, 819–835. <http://www.crab.rutgers.edu/~nb361/mypapers/Kent1978.pdf>.
91. Bou-Rabee, N.; Donev, A.; Vanden-Eijnden, E. Metropolized integration schemes for self-adjoint diffusions. <http://www.crab.rutgers.edu/~nb361/mypapers/BoDoVa2013.pdf>, 2013
92. Bou-Rabee, N.; Owhadi, H. Long-Run Accuracy of Variational Integrators in the Stochastic Context. *SIAM J Numer Anal* **2010**, *48*, 278297.
93. Ezra, G.S. Reversible measure-preserving integrators for non-Hamiltonian systems. *J Chem Phys* **2006**, *125*, 034104. [http://jcp.aip.org/resource/1/jcpsa6/v125/i3/p034104\\_s1](http://jcp.aip.org/resource/1/jcpsa6/v125/i3/p034104_s1).
94. Bussi, G.; Parrinello, M. Accurate Sampling using Langevin Dynamics. *Phys Rev E* **2007**, *75*, 056707.
95. Shardlow, T. Splitting for dissipative particle dynamics. *SIAM J. Sci. Comput.* **2003**, *24*, 12671282.
96. Serrano, M.; De Fabritiis, G.; Espanol, P.; Coveney, P.V. A stochastic Trotter integration scheme for dissipative particle dynamics. *Math. Comput. Simulat.* **2006**, *72*, 190–194.
97. Pavliotis, G.A.; Stuart, A.M.; Zygalakis, K.C. Calculating Effective Diffusivities in the Limit of Vanishing Molecular Diffusion. *J Comput Phys* **2008**, *228*, 1030–1055.
98. van Gunsteren, W.F.; Berendsen, H.J.C. Algorithms for Brownian Dynamics. *Mol Phys* **1982**, *45*, 637–647.

99. Nummelin, E. *General Irreducible Markov Chains and Non-negative Operators*; Cambridge University Press: New York, NY, 1984.
100. Tierney, L. Markov Chains for Exploring Posterior Distributions. *Ann Stat* **1994**, *22*, 1701–1728.
101. Evans, L. An Introduction to Stochastic Differential Equations. Lecture Notes Version 1.2, 2007
102. Gelman, A.; Gilks, W.R.; Roberts, G.O. Weak convergence and optimal scaling of random walk Metropolis algorithms. *Ann Appl Probab* **1997**, *7*, 110–120.
103. Roberts, G.O.; Rosenthal, J.S. Optimal Scaling of Discrete Approximations to Langevin Diffusions. *J Roy Statist Soc Ser B* **1998**, *60*, 255–268.
104. Beskos, A.; Roberts, G.O.; Stuart, A.M. Optimal scalings for local Metropolis-Hastings chains on non-product targets in high dimensions. *Ann Appl Probab* **2009**, *19*, 863–898. <http://projecteuclid.org/euclid.aoap/1245071013>.
105. Beskos, A.; Pillai, N.S.; Roberts, G.O.; Sanz-Serna, J.M.; Stuart, A.M. Optimal Tuning of Hybrid Monte-Carlo algorithm. To appear in *Bernoulli*
106. Mattingly, J.C.; Pillai, N.S.; Stuart, A.M. Diffusion Limits of the Random Walk Metropolis Algorithm in High Dimensions. *Ann Appl Probab* **2012**, *22*, 881–930.
107. Kang, F.; Dao-Liu, W. Dynamical systems and geometric construction of algorithms. *Computational Mathematics in China. Contemporary Mathematics. AMS* **1994**, *163*, 1–32.

© 2013 by the author; licensee MDPI, Basel, Switzerland. This article is an open access article distributed under the terms and conditions of the Creative Commons Attribution license (<http://creativecommons.org/licenses/by/3.0/>).